Subcutaneous Fat Tissue Density as a Novel Diagnostic Indicator in Distinguishing Pulmonary Edema from Viral Pneumonias

Pulmoner Ödem ile Viral Pnömoniyi Ayırt Etmede Yeni Bir Tanısal Gösterge Olarak Deri Altı Yağ Dokusu Yoğunluğu

Zeynep ATÇEKEN[a], Yüksel PEKER[b,c,d,e], Mahir KAPMAZ[f], Hüseyin Ekin ERGİN[a], Kayhan Çetin ATASOY[a]

[a]Koç University Faculty of Medicine, Department of Radiology, İstanbul, Türkiye
[b]Koç University Faculty of Medicine, Department of Pulmonary Medicine, İstanbul, Türkiye
[c]Gothenburg University, Sahlgrenska Academy, Institute of Medicine, Department of Molecular and Clinical Medicine/Cardiology, Gothenburg, Sweden
[d]Pittsburgh University Faculty of Medicine, Division of Pulmonary, Allergy, and Critical Care Medicine, Pittsburgh, PA, USA
[e]Lund University Faculty of Medicine, Department of Clinical Sciences, Respiratory Medicine and Allergology, Lund, Sweden
[f]Medipol University Faculty of Medicine, Department of Infectious Diseases, İstanbul, Türkiye

ABSTRACT Objective: Diffuse pulmonary opacities are seen in both pulmonary edema (PE) and pulmonary infections such as viral pneumonia (VP) and *Pneumocystis jirovecii* pneumonia (PJP), and distinguishing these from each other might be challenging. We aimed to show whether subcutaneous fat tissue density (SFTD) measurement in computed tomography scans helps to distinguish PE from VP and PJP. **Material and Methods:** In this retrospective study, SFTD, defined in terms of Hounsfield unit (HU) was evaluated in computed tomography scans of 99 patients with PE, 103 patients with VP and PJP, and 110 healthy individuals. The SFTD was calculated by using a region of interest with a diameter of approximately 1 cm in the subcutaneous adipose tissue, located 3 cm superior-inferior and medial-lateral to the junction of the midclavicular line and the xiphoid tip on the chest wall, blinded to the clinical data. **Results:** Median SFTD was -82.5 HU [interquartile range (IQR) -88.7; -67.4] in patients with PE, -117.7 HU (IQR -121.3; -111.8) in patients with VP and PJP, and -120.3 HU (IQR -123.1; -117.0) in the control group (p<0.001). All patients with PE had SFTD at least -95 HU. None of the patients with VP and PJP as well as controls had SFTD less than -101 HU. **Conclusion:** Our results suggest that a SFTD measurement above -95 HU might be useful in differentiating PE from pneumonia in patients with diffuse lung opacities.

Keywords: Subcutaneous fat tissue density; pulmonary edema; pulmonary infection; chest CT

ÖZET Amaç: Diffüz pulmoner opasiteler, hem pulmoner ödem (PÖ) hem de viral pnömoniler (VP) ile *Pneumocystis jirovecii* pnömonisi (PJP) gibi pulmoner enfeksiyonlarda görülür ve bu durumların birbirinden ayırt edilmesi radyolojik olarak zor olabilir. Bu çalışmada, toraks bilgisayarlı tomografi görüntülerinde yaygın akciğer opasiteleri olan hastalarda subkütan yağ dokusu dansitesini (SYDD) ölçerek, PÖ'yü, VP ve PJP'lerden ayırt etmeyi amaçladık. **Gereç ve Yöntemler:** Retrospektif olarak gerçekleştirilen bu çalışmada SYDD, Hounsfield birimi [Hounsfield unit (HU)] cinsinden tanımlandı; PÖ'lü 99 hasta, VP ve PJP'li 103 hasta ile 110 sağlıklı bireyin bilgisayarlı tomografi görüntüleri incelendi. SYDD ölçümleri, klinik bilgiler bilinmeden, midklavikular çizgi ile ksifoid çıkıntının birleşim noktasından 3 cm superior-inferior ve mediyal-lateral olarak göğüs duvarındaki subkütan yağ dokusunda, yaklaşık 1 cm çapında bir ilgi alanı kullanılarak hesaplandı. **Bulgular:** Medyan SYDD, PÖ hastalarında -82,5 HU [güven aralığı (GA) -88,7; -67,4], VP ve PJP hastalarında -117,7 HU (GA -121,3; -111,8), kontrol grubunda ise -120,3 HU (GA -123,1; -117,0) olarak bulundu (p<0,001). PÖ hastalarının tamamında, SYDD en az -95 HU idi. Pnömoni hastalarında ve kontrol grubunda ise SYDD hiçbir hastada -101 HU'dan büyük değildi. **Sonuç:** Sonuçlarımız, yaygın akciğer opasitesi olan hastalarda -95 HU'dan büyük SYDD değerlerinin, PÖ'yü VP ile PJP'den ayırt etmede faydalı bir gösterge olabileceğini düşündürmektedir.

Anahtar Kelimeler: Subkütan yağ dokusu dansitesi; pulmoner ödem; pulmoner enfeksiyon; toraks BT

Ground-glass opacity (GGO) is a common finding in chest computed tomography (CT). It involves a broad spectrum of differential diagnoses in the acute setting, including viral pneumonias (VPs) due to a variety of agents including influenza, coronavirus disease-2019 (COVID-19) and cytomegalovirus (CMV), in addition to *Pneumocystis jirovecii* pneumonia (PJP) and non-infectious conditions such as vaping-related lung injury, alveolar hemorrhage, and pulmonary edema (PE).[1] GGO may be nonspecific, and differentiating those conditions from each other is crucial since they all need different treatments.

Radiodensity of fat tissue can be quantitatively measured through CT in Hounsfield units (HU).[2] CT-derived average adipose tissue radiodensity has been established as an indirect marker for adipose tissue quality.[3] HU is not only an indicator of stored triglycerides in adipose tissue but it also represents other components of tissue structures, including water.[4-6]

In the current study, we aimed to measure subcutaneous fat tissue density (SFTD) in CT scans of the patients with PE, VP and PJP as well as healthy controls in order to determine a possible cut-off HU value for distinguishing PE from VP.

MATERIAL AND METHODS

PARTICIPANTS

This study was a double-center (Koç University Hospital and Koç Healthcare American Hospital, İstanbul), retrospective evaluation of a clinical cohort between March 2020-February 2024. In all, 312 randomly selected adults who underwent chest CT examinations comprised the final study population: 99 patients with clinically and radiologically confirmed PE, 103 patients diagnosed as VP or PJP, based on the clinical and laboratory results, and 110 healthy controls (Figure 1). The patient group was randomly selected from the CT-scan list with preliminary differential diagnosis PE or VP, including COVID-19, and PJP. The healthy control group were patients referred for check-up examination. Patients having both PE and VP or PJP as well as the ones with other pulmonary diseases which may affect the lung parencyma (interstitial lung disease, tuberculosis, lung cancer) were excluded.

The study was conducted in accordance with the Declaration of Helsinki. The Koç University Committee on Human Research approved the study pro-
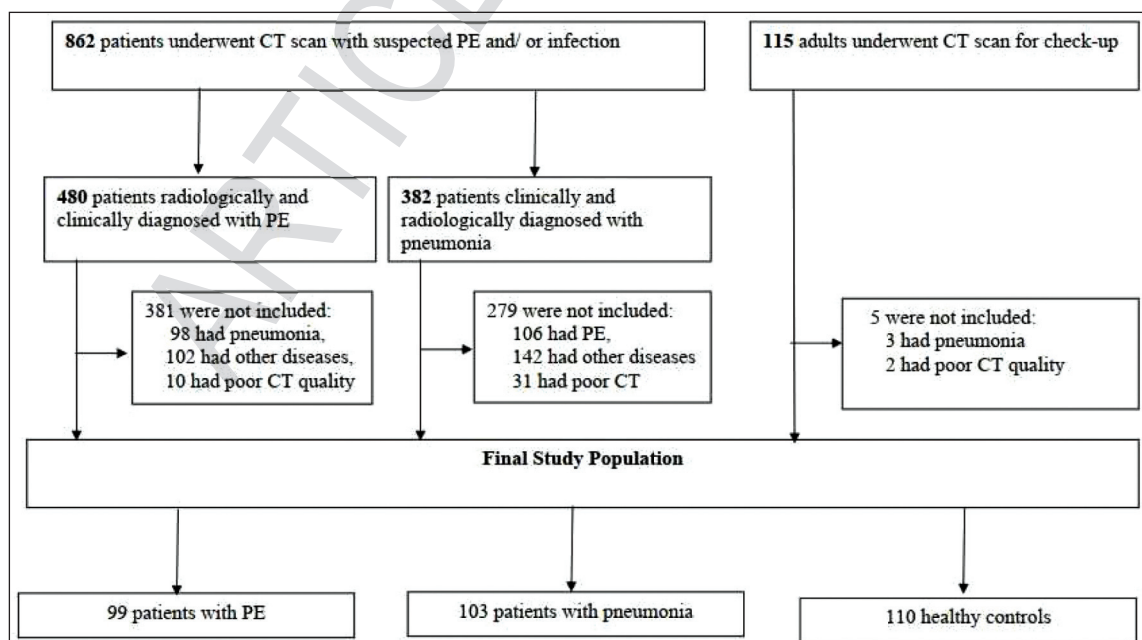

FIGURE 1: Flow-chart of the study population. CT: Computed tomography; PE: Pulmonary edema

tocol (date: December 26, 2024; no: 2024.456.IRB2. 197). Written informed consent was obtained from all the subjects involved in this study.

CLASSIFICATION OF THE GROUPS

The radiological diagnostic criteria for PE included vascular engorgement and bronchovascular bundle thickness due to lymphatic engorgement, and inter-lobular septal thickening, which suggested interstitial edema.[7] While GGO were seen in early cases, consolidation was seen in cases of advanced alveolar flooding . Pleural effusions and an enlarged heart are additional features of cardiogenic PE.[8]

In the VP cases, the diagnosis of influenza pneumonia was based on a) the presence of community-acquired pneumonia detected positive for influenza A or B real-time polymerase chain reaction (PCR) and/or antigen on nasopharyngeal swabs, and b) a serum procalcitonin level lower than 0.25 ng/mL, and a low suspicion for bacterial co-infection.[9,10]

The diagnosis of COVID-19 pneumonia was based on positive severe acute respiratory syndrome-coronavirus-2 PCR testing of nasopharyngeal swabs taken in the previous 14 days prior to hospital admission from patients who arrived with acute respiratory symptoms and/or body temperature higher than 37.5 ˚C.[11] CMW pneumonia was diagnosed with a positive CMV PCR test in plasma or bronchoalevolar lavage (BAL), and the absence of any explanation for the respiratory symptoms.[12,13] PJP was confirmed by positive immunofluorescence staining on BAL or tissue samples or PCR assay on respiratory specimens.[13]

Demographic data, comorbidities (hypertension, Type 2 diabetes mellitus), clinical symptoms, laboratory and radiological findings, treatment, and outcomes were collected prospectively from electronic health records.

CHEST COMPUTED TOMOGRAPHY PROTOCOL AND ASSESSMENT

All patients underwent scanning using a 64-detector row CT scanner (Somatom® Definition AS; Siemens Healthineers, Forchheim, Germany). All chest CT scans were obtained using standardized protocols, with patients in the supine position during end-inspiratory breath-hold. To decrease the radiation dose as low as reasonably possible X-ray tube parameters were selected automatically by the scanner depending on patient size. No contrast material was administered.

SFTD was measured in HU using a region of interest (ROI) on mediastinal window settings (window width: 350 HU, window level: 50 HU), which do not allow visualization of parenchymal findings. The ROI was defined as a circle with a 1 cm diameter located within the subcutaneous fat tissue, 3 cm superior-inferior and medial-lateral to the junction of the midclavicular line and the xiphoid tip on the chest wall. Skin, breast, any muscles or fibrous tissues as well as artifacts were excluded from measurements. Two examples from cases with COVID-19 pneumonia and PE are illustrated in Figure 2.

All measurements were done by the same observer (ZA) blinded to the clinical data including preliminary diagnosis. Each measurement was repeated 3 times (with a 1-month interval) to minimize variations and ensure the reliability of the results, and the mean of the 3 measurements was obtained.

STATISTICS

Baseline demographics were summarized as mean with standard deviation or median with 25th and 75th
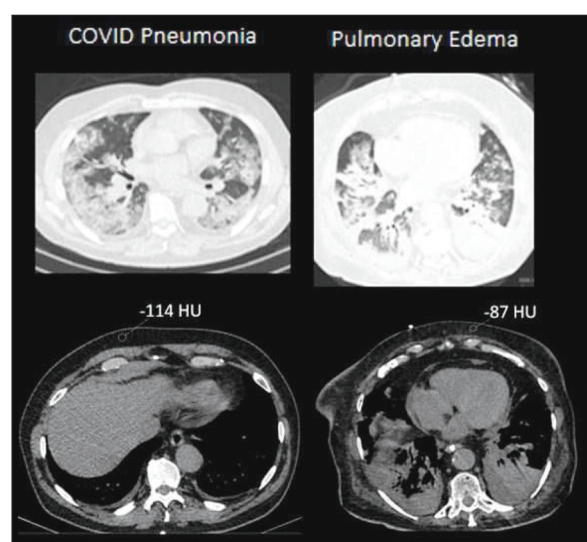
FIGURE 2: Parenchymal ground-glass opacities and consolidations of 2 patients with COVID-19 pneumonia (upper right panel) and pulmonary edema (upper left panel), and subcutaneous fat tissue density measurements (lower right panel vs. lower left panel)
COVID-19: Coronavirus disease-2019; HU: Hounsfield unit

percentile for the continuous variables, and as count with percentage for the categorical variables. Shapiro-Wilk test was used to test normality assumption. For the continuous variables, the differences between groups was tested via Kruskal-Wallis test while the "post hoc" analysis was run using the Mann-Whitney U test with a Bonferroni correction. For the categorical variables, chi-square test or Fisher's exact test was applied. Intraobserver variability for the repeated SFTD measurements was evaluated by the intraclass correlation coefficient (ICC). The linear regression analysis was conducted to examine the association between PE diagnosis and SFTD measurements adjusted for age, sex, body mass index (BMI), diabetes mellitus and hypertension. Participants were coded as PE: 1, pneumonia: 2, and healthy controls: 3. The accepted significance level for all tests was set as 5%, and statistical analyses were performed using IBM SPSS 28.0 for Windows SPSS Inc., Chicago, Illinois, USA.

RESULTS

As illustrated in Figure 1, a total of 862 patients had the preliminary or differential diagnosis PE and/or pneumonia on the CT scans. Among 480 patients with PE, 381 were not included due to concomitant pneumonia or other lung diseases or poor CT quality. Similarly, among 382 patients with pneumonia, 279 were excluded due to concomitant PE or other lung diseases or poor CT quality. Thus, 202 participants comprised the patient group. Of 115 adults undergoing CT scans for check-up, five were excluded due to pneumonia or poor CT quality, and 110 participants comprised the healthy controls.

Thus, 312 participants (48.7% males) with a mean age of 61.5 (SD=17.9) years were included in the current study. The mean BMI was 26.5±4.9 and 21.4% of the entire population were obese. As shown in Table 1, the patients in the PE group were significantly older and had higher occurrence of hypertension and diabetes mellitus than the other groups.

The intraobserver reliability analysis demonstrated excellent ICC among the measurements, with a Cronbach's alpha value of 0.991. The mean and standard deviation for each variable were as follows:

	PE (n=102)	VP or PJP (n=100)	Controls (n=110)	p value
TABLE 1: Baseline demographics and clinical characteristics of the study groups				
Age (years) (X̄±SD)	78.7±11.6	59.8±13.8	47.5±12	<0.001
BMI (X̄±SD)	25.8±4.7	26.7±4.9	26.8±5.2	0.305
Male sex, %	44 (43%)	51 (51%)	57 (52%)	0.39
Obesity, %	25 (47.2%)	16 (30.2%)	12 (22.6%)	0.42
Hypertension	61 (59.8%)	40 (40%)	15 (13.6%)	<0.001
Diabetes mellitus	33 (32.4%)	24 (24%)	7 (6.4%)	<0.001

PE: Pulmonary edema; VP: Viral pneumonia; PJP: *Pneumocystis jirovecii* pneumonia; SD: Standard deviation; BMI: Body mass index

HU1 (-104.30±22.56), HU2 (-105.40±22.47), and HU3 (-105.18±22.21). Fleiss multirater kappa analysis revealed a kappa value of 0.018 (standard error=0.006, z=3.234, p<0.001), indicating statistically significant intraobserver agreement. The 95% confidence interval for the kappa statistic ranged from 0.007 to 0.029.

The SFTD measurements across the 3 groups have been presented in Figure 3. Median SFTD was -82.5 HU [interquartile range (IQR) -88.7; -67.4] in patients with PE, -117.7 HU (IQR -121.3; -111.8) in patients with VP and PJP, and -120.3 HU (IQR -123.1; -117.0) in the control group (p<0.001). The minimum SFTD value in patients with PE was -95 HU, whereas the maximum SFTD value in patients with pneumonia and control group was -101 HU.

As presented in Table 2, cardiomegaly, left atrium enlargement, pleural effusion, bronchial wall
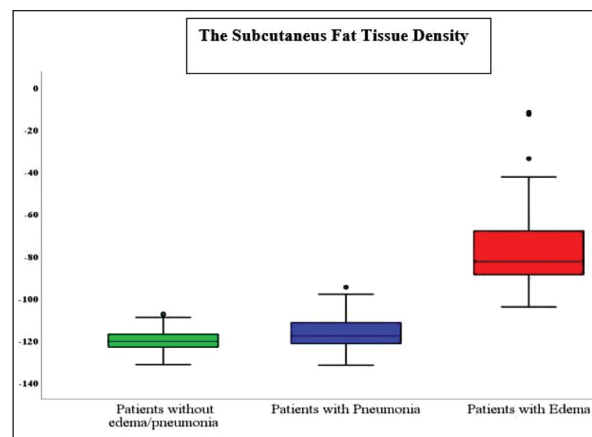
FIGURE 3: Distribution of the subcutaneous fat tissue density measurement across the study groups. Control vs. pneumonia (p=0.012), control vs. pulmonary edema (p<0.001), and pneumonia vs. pulmonary edema (p<0.001)

TABLE 2: Proportion of the clinically meaningful radiological findings across the patient groups

	PE (n=102)	VP or PJP (n=100)	p value
Cardiomegaly, %	87.3	19.0	<0.001
Left atrium enlargement, %	77.5	16.0	<0.001
Pleural effusion, %	88.2	27.0	<0.001
Bronchial wall thickening, %	98.0	27.0	<0.001
Interlobular septal thickening, %	99.0	27.0	<0.001

PE: Pulmonary edema; VP: Viral pneumonia; PJP: *Pneumocystis jirovecii* pneumonia

TABLE 3: Association of the occurrence of PE and the subcutaneous fat tissue density

	Unstandardized coefficients β	95% confidence interval for β		p value
		Lower	Upper	
PE	21.13	18.206	24.055	<0.001
Age	0.013	-0.141	0.168	0.865
BMI	-0.313	-0.666	0.039	0.081
Male sex	0.196	-.3.309	3.701	0.912
Hypertension	-0.329	-4.840	4.181	0.886
Diabetes mellitus	-0.826	-5.577	3.926	0.732

PE: Pulmonary edema; BMI: Body mass index

thickening, and interlobular septal thickening were significantly more frequent in patients with PE compared to patients with VP and PJP.

The results of the linear regression analysis are shown in Table 3. The analysis showed that the association between PE and SFTD in HU was statistically significant.

DISCUSSION

The main finding of our study was that SFTD in patients with PE was significantly higher than in patients with VP and healthy controls, and a SFTD value above -95 HU might be a useful indicator for differentiating PE from VP and PJP.

To our best knowledge, this is the first study that assesses SFTD values in healthy controls and disease states and uses this finding for differentiating PE from pneumonias. Our findings support that a SFTD threshold of -95 HU can accurately distinguish PE from viral and *Pneumocystis* pneumonias, which may both present with diffuse GGOs on CT.

Differentiating PE from conditions like COVID-19 pneumonia or acute viral infections is a significant challenge due to overlapping radiological features, including GGO and consolidations. According to a study by Cozzi et al., a more comprehensive approach is necessary for an appropriate diagnosis because GGO is an imaging feature that can be seen in conditions including vasculitis, pneumonia, alveolar hemorrhage, and PE.[14] Similarly, Marginean at al. emphasized that radiologists often experience difficulties in differentiating COVID-19 pneumonia from other causes of lung opacities, especially in the absence of distinctive imaging patterns.[15] Plasencia Martínez and colleagues, investigated conditions that presented with multifocal lung opacities which can be mistaken for pneumonia.[16] They emphasized the need for integrating specific imaging markers to improve diagnostic accuracy for multifocal lung opacities. Although conventional findings such as cardiomegaly and vascular congestion are helpful in the diagnosis of PE, we propose that the inclusion of SFTD measurements could provide a reproducible quantitative parameter that overcomes the limitations of conventional differential diagnostic approach.

Fat tissue radiodensity, as measured in HU, reflects blood flow, lipid content and fluid to triglyceride ratio.[4-6] We believe the increased chest wall SFTD in patients with PE results from increased fluid in the subcutaneous fat, causing higher fluid to triglyceride ratio. Increased SFTD, particularly in PE, may directly reflect elevated fluid accumulation within the tissue, whether interstitial or alveolar in nature. The HU value of adipose tissue is influenced by the relative proportions of water, triglycerides, and cellular components. In PE, elevated systemic venous pressure leads to fluid accumulation not only within the pulmonary parenchyma but also in systemic tissues. This results in increased water content in subcutaneous fat and, consequently, higher HU values.[4-6] In contrast, such systemic fluid overload is typically absent in infectious conditions such as VP or PJP; in fact, tissue density may even be lower in some patients due to hypovolemia or the effects of inflammatory processes.[2,3]

Our results showed the SFTD in patients with PE was significantly higher than the patients with VP

and healthy controls. Of note, all patients with PE had SFTD at least -95 HU, and none of the patients with VP and PJP as well as controls had SFTD more than -101 HU. Thus, these findings suggest that SFTD might be a PE-specific novel indicator in the differential diagnosis of distinguishing PE from VP and PJP.

While this research shows promise it also comes with some limitations that need consideration. The retrospective approach used in the study could lead to selection bias. Although the -95 HU cut-off effectively differentiated patients with PE from those with VP and healthy controls, this threshold may exhibit variability across different scanner models and imaging protocols. We acknowledge that the -95 HU cut-off value should be re-evaluated in different clinical populations. Future studies with a multicenter and prospective design, supported by automated image processing algorithms are warranted to validate our findings. In such settings, receiver operating characteristic analysis would allow for a more accurate determination of the optimal balance between sensitivity and specificity. Additionally, even though SFTD has shown specificity for PE in this investigation, more studies are needed to confirm its effectiveness in a setting with larger clinical groups and in different systemic diseases.

CONCLUSION

In conclusion, the measurement of SFTD represents a novel and quantifiable tool for differentiating PE from VPs in patients with diffuse lung opacities on CT. Incorporating this parameter into clinical practice might enhance the diagnostic accuracy and improve patient management, particularly in cases with overlapping imaging features.

Conflict of Interest

No conflicts of interest between the authors and / or family members of the scientific and medical committee members or members of the potential conflicts of interest, counseling, expertise, working conditions, share holding and similar situations in any firm.

Authorship Contributions

Idea/Concept: *Zeynep Atçeken, Kayhan Çetin Atasoy;* ***Design:*** *Zeynep Atçeken, Yüksel Peker, Kayhan Çetin Atasoy;* ***Control/Supervision:*** *Yüksel Peker, Kayhan Çetin Atasoy;* ***Data Collection and/or Processing:*** *Zeynep Atçeken, Mahir Kapmaz, Hüseyin Ekin Ergin;* ***Analysis and/or Interpretation:*** *Zeynep Atçeken, Yüksel Peker, Mahir Kapmaz, Hüseyin Ekin Ergin, Kayhan Çetin Atasoy;* ***Literature Review:*** *Zeynep Atçeken;* ***Writing the Article:*** *Zeynep Atçeken, Yüksel Peker;* ***Critical Review:*** *Yüksel Peker, Mahir Kapmaz, Hüseyin Ekin Ergin, Kayhan Çetin Atasoy;* ***References and Fundings:*** *Kayhan Çetin Atasoy;* ***Materials:*** *Zeynep Atçeken, Hüseyin Ekin Ergin, Kayhan Çetin Atasoy;* ***Other:*** *Zeynep Atçeken, Yüksel Peker, Mahir Kapmaz, Hüseyin Ekin Ergin, Kayhan Çetin Atasoy.*

REFERENCES

1. Matos MJ, Rosa ME, Brito VM, Amaral LT, Beraldo GL, Fonseca EK, et al. Differential diagnoses of acute ground-glass opacity in chest computed tomography: pictorial essay. einstein (São Paulo). 2021;19:eRW5772. https://www.scielo.br/j/eins/a/63XjZvQsqzBTZDfmmnYVQ4q/?format=pdf&lang=en

2. Ebadi M, Dunichand-Hoedl AR, Rider E, Kneteman NM, Shapiro J, Bigam D, et al. Higher subcutaneous adipose tissue radiodensity is associated with increased mortality in patients with cirrhosis. JHEP Rep. 2022;4(7):100495. PMID: 35600667; PMCID: PMC9117882

3. Hanley C, Shields KJ, Matthews KA, Brooks MM, Janssen I, Budoff MJ, et al. Associations of cardiovascular fat radiodensity and vascular calcification in midlife women: The SWAN cardiovascular fat ancillary study. Atherosclerosis. 2018;279:114-21. PMID: 30241697; PMCID: PMC6295258

4. Gifford A, Walker RC, Towse TF, Brian Welch E. Correlations between quantitative fat-water magnetic resonance imaging and computed tomography in human subcutaneous white adipose tissue. J Med Imaging (Bellingham). 2015;2(4):046001. PMID: 26702407; PMCID: PMC4684077

5. Weyer C, Foley JE, Bogardus C, Tataranni PA, Pratley RE. Enlarged subcutaneous abdominal adipocyte size, but not obesity itself, predicts type II diabetes independent of insulin resistance. Diabetologia. 2000;43(12):1498-506. PMID: 11151758

6. Baba S, Jacene HA, Engles JM, Honda H, Wahl RL. CT Hounsfield units of brown adipose tissue increase with activation: preclinical and clinical studies. J Nucl Med. 2010;51(2):246-50. PMID: 20124047

7. Barile M. Pulmonary edema: a pictorial review of imaging manifestations and current understanding of mechanisms of disease. Eur J Radiol Open. 2020;7:100274. PMID: 33163585; PMCID: PMC7607415

8. Assaad S, Kratzert WB, Shelley B, Friedman MB, Perrino A Jr. Assessment of pulmonary edema: principles and practice. J Cardiothorac Vasc Anesth. 2018;32(2):901-14. PMID: 29174750 doi:10.1016/j.jvca.2017.09.026

9. Merckx J, Wali R, Schiller I, Caya C, Gore GC, Chartrand C, et al. Diagnostic accuracy of novel and traditional rapid tests for influenza infection compared with reverse transcriptase polymerase chain reaction: a systematic review and meta-analysis. Ann Intern Med. 2017;167(6):394-409. PMID: 28869986

10. Vos LM, Bruning AHL, Reitsma JB, Schuurman R, Riezebos-Brilman A, Hoepelman AIM, et al. Rapid molecular tests for influenza, respiratory syncytial virus, and other respiratory viruses: a systematic review of diagnostic accuracy and clinical impact studies. Clin Infect Dis. 2019;69(7):1243-53. PMID: 30689772; PMCID: PMC7108200

11. Msemburi W, Karlinsky A, Knutson V, Aleshin-Guendel S, Chatterji S, Wakefield J. The WHO estimates of excess mortality associated with the COVID-19 pandemic. Nature. 2023;613(7942):130-7. PMID: 36517599; PMCID: PMC9812776

12. Ljungman P, Boeckh M, Hirsch HH, Josephson F, Lundgren J, Nichols G, et al; Disease Definitions Working Group of the Cytomegalovirus Drug Development Forum. Definitions of cytomegalovirus infection and disease in transplant patients for use in clinical trials. Clin Infect Dis. 2017;64(1):87-91. PMID: 27682069 doi:10.1093/cid/ciw855

13. Lagrou K, Chen S, Masur H, Viscoli C, Decker CF, Pagano L, et al. Pneumocystis jirovecii disease: basis for the revised EORTC/MSGERC invasive fungal disease definitions in individuals without human immunodeficiency virus. Clin Infect Dis. 2021;72(Suppl 2):S114-20. PMID: 33709126; PMCID: PMC8243279

14. Cozzi D, Cavigli E, Moroni C, Smorchkova O, Zantonelli G, Pradella S, et al. Ground-glass opacity (GGO): a review of the differential diagnosis in the era of COVID-19. Jpn J Radiol. 2021;39(8):721-32. PMID: 33900542; PMCID: PMC8071755

15. Marginean CM, Popescu M, Vasile CM, Cioboata R, Mitrut P, Popescu IAS, et al. Challenges in the Differential Diagnosis of COVID-19 Pneumonia: A Pictorial Review. J Clin Med. 2021;10(8):1731. doi:10.3390/jcm10081731

16. Plasencia Martínez JM. Schematic approach to the diagnosis of multifocal lung opacities in the emergency department. Radiologia (Engl Ed). 2023;65 Suppl 1:S63-72. PMID: 37024232 doi:10.1016/j.rx.2022.09.004